Longitudinal phase space coating of beam in a storage ring

C. M. Bhat

Accelerator Division, Fermi National Accelerator Laboratory,

P. O. Box 500, Batavia, IL 60510, USA

(Draft)

(To be submitted to PLA)

Abstract:

In this letter, I describe a scheme for beam stacking in a storage ring using barrier buckets without any emittance dilution to the majority of the beam. First I discuss the general principle of the method "longitudinal phase-space coating". This scheme has been convincingly validated by multi-particle 2D-beam dynamics simulations and has been demonstrated with beam experiments at the Fermilab Recycler. We also present its usefulness in mapping the incoherent synchrotron tune spectrum of beam particles in barrier buckets and to produce a clean hollow beam in longitudinal phase space. The beam stacking scheme presented here is the first of its kind.

I. Introduction

High intensity hadron and ion beam stacking with no emittance dilution in a synchrotron is one of the major problems for the past several decades. Considerable research has been undertaken at many accelerator complexes over the years to develop novel stacking methods [1], viz. *box-car* stacking [2], slip stacking [3], momentum stacking and cooling [4], stacking using double harmonic rf systems [5] , transverse and longitudinal phase-space painting [6]. The first three of these use resonant rf systems and the last one is mostly used while beam stacking from a linear accelerator to a storage ring. Each one of them has its merits and limitations. The Recycler Ring at Fermilab [7], an 8 GeV antiproton storage ring, uses *barrier rf* technology [8] in all of its beam manipulations, unlike any storage rings in the world. Therefore none of the methods of beam stacking mentioned earlier could have been used in the Recycler Ring without major rf modifications. Further advancement in beam stacking was inevitable for the Fermilab Recycler operation.

The use of barrier buckets for rf manipulations in synchrotron accelerators and in storage rings is relatively a new to the technology. Significant theoretical as well as experimental research have been undertaken during the past two decades [8-16]. Use of barrier rf buckets are foreseen in future new accelerator facilities [17].

Till very recently the Recycler was in use as the primary antiproton depository at the Fermilab accelerator complex. During normal antiproton stacking, ~20×10^{10} antiprotons with longitudinal emittance (LE) <13 eV s was extracted from the Fermilab Accumulator Ring and transferred to the Recycler. The new beam then is added to the initial *cold beam* which was in another rectangular barrier bucket in the Recycler. This sequence of beam transfer is repeated several times in a day until the Recycler antiproton stack was enough to fill the Tevatron for collider operation. The entire stack of the Recycler is cooled using stochastic cooling and electron cooling between the antiproton transfers.

Over the past several years, a number of improvements have been made in antiproton stacking schemes in the Recycler [14]. A scheme involving *morphing* of barrier rf pulses [15] was the last improvement. All of these schemes involved non-adiabatic collapsing of barrier bucket containing the cold beam at the time of adding the new beam to the stack that resulted in

longitudinal emittance growth of about 15% per transfer. In the case of multiple beam transfers, the overall emittance growth is as high as 50%. The disadvantages of all the early stacking schemes described in refs. 14 and 15 were that a) the initial cold beam is disturbed significantly every time a non-adiabatic barrier collapsing took place and b) the momentum spreads of the new beam and that of the initial beam have to be matched each time before merging.

In this letter I present a scheme of beam stacking "longitudinal phase-space coating" (LPSC) [18]. The method of LPSC explained here is different from longitudinal phase space painting explained in the literature [6]. Here the 6D emittance of the original cold beam can be held unchanged for a number of consecutive beam transfers from upstream machine and the emittance growth for the newly arrived beam is minimal. Presence of barrier rf buckets in the ring is critical to use this novel technique. LPSC can be viewed as the reverse of "longitudinal momentum mining" [13]. We illustrate working principle and an experimental demonstration of the LPSC using nearly rectangular barrier pulses though beam stacking illustrated here is independent of the barrier rf waveform illustrated in ref. 9.

II. Principle of Longitudinal Phase-space Coating

A barrier rf bucket in a synchrotron is generated either by using a very broad band rf system or by a set of fast kickers which produce a minimum three regions per revolution period T_0 namely a region with positive and negative voltage barriers with a zero voltage region in the pulse gap. Longitudinal dynamics of a charged particle in such a rf bucket is characterized by its energy offset ΔE from synchronous energy E_0 and a relative time coordinate with respect to an arbitrarily chosen fixed point. Such a particle will continue to slip relative to a synchronous particle in the region with zero rf voltage in a barrier bucket. It will lose or gain energy as soon as it encounters a barrier pulse and this will continue till there is enough kick from the barrier pulse to change its direction of slip. Thus, the barrier buckets sets the particles into synchrotron oscillations. The motion of any particle in a synchrotron is governed by [9],

$$\frac{d\tau}{dt} = -\eta \frac{2\pi\Delta E}{T_0 \beta^2 E_0} \quad \text{and} \quad \frac{d(\Delta E)}{dt} = \frac{eV(\tau)}{T_0} \tag{1}$$

The quantities e, η and β are electronic charge, phase slip factor and the ratio of the particle velocity to that of light, respectively. $-\tau$ is the time difference between the arrival of the particle and that of a synchronous particle at the center of the rf bucket. $V(\tau)$ is the amplitude of

the rf voltage waveform. From Eqs. (1) we can obtain the general Hamiltonian for synchrotron motion for an arbitrary barrier rf wave form as,

$$H(\tau,\Delta E) = -\frac{\eta}{2\beta^2 E_0}\Delta E^2 - \frac{e}{T_0}\int_0^{\tau} V(t)dt \qquad (2)$$

The second term in the above equation represents the potential energy of the particle. It can be shown that the maximum value of the energy offset, $\hat{\Delta E}$, of a particle during its synchrotron motion in a barrier bucket is related to its penetration depth $\hat{T}$ by

$$\hat{\Delta E} = \sqrt{\frac{2\beta^2 E_0}{|\eta| T_0}\left|\int_{T_2/2}^{T_2/2+\hat{T}} eV(t)dt\right|} \qquad (3)$$

with T_2 equals the pulse gap. The $\hat{\Delta E}$ represents the bucket height when $\hat{T}$ is the total width of the barrier pulse. For a rectangular barrier bucket one can replace $\int_{T_2/2}^{T_2/2+\hat{T}} eV(t)dt = eV_0\hat{T}$ which simplifies significantly. Consequently, it is easy to imagine that a rectangular barrier bucket can be looked upon as one or more barrier buckets one inside the other, so that one of the inner one confines all the particles whose maximum energy offset is below $\hat{\Delta E}$ with a clear boundary.

The principal goal of the LPSC is to isolate particles of certain maximum energy spread using a *mini-barrier* bucket. Coat the injected beam on the top of the isolated particles. The coating takes place in $(\Delta E, \Delta t)$ –space. The particles in the mini-bucket will be left undisturbed throughout the stacking.

A schematic view of the rf wave forms with the beam phase space boundary (closed contour in left figure) and the corresponding potential well, representing beam particles for a storage ring operating below transition energy is shown in Fig.1. The scheme can be looked upon as a set of four steps of rf gymnastics for every beam transfer. The initial beam distribution is shown in Fig. 1(a). The region intended not to be affected during painting is also shown in Fig. 1(a) (left, indicated by denser region of phase space). Before the transfer of new beam a mini-bucket made of two barrier pulses "3" and "4" is adiabatically opened as shown in Fig. 1(b). The barrier pulse width and height are chosen to be T_m and V_m each, respectively.

Thus the mini-bucket isolates particles in a phase space area $\varepsilon_m = T_m \Delta E_m + T_0 |\eta| \Delta E_m{}^3 / \left[6\beta^2 E_0 e V_m\right]$ close to the synchronous energy. In an ideal case, one can capture entire stack of initial beam in the mini-bucket. Subsequently new beam is injected in a separate barrier bucket made of rf pulses "5" and"6". The barrier pulses "2" and "5" removed to coat the injected beam as shown in Fig.1(c) and rf pulse "6" is moved to the location of "2" adiabatically to complete coating as shown in Fig. 1(d). As a consequence of this rf gymnastic the total energy spread of the injected beam will decrease initially though their potential energy is higher than that in the mini-bucket. During this stage the particles which are outside the mini-barrier bucket mix well with the newly arrived particles and performing synchrotron oscillations without affecting the beam particles in the mini-barrier bucket.

III. Experimental Demonstration of LPSC scheme at the Fermilab Recycler

The LPSC method of beam stacking is applied to the beam in the Fermilab Recycler [7]. The Recycler is an 8 GeV permanent magnet synchrotron storage ring that operates below the transition energy (γ_T = 21.6) and has T_0 = 11.12 μsec. The Recycler was used as the primary antiproton storage ring for the proton-antiproton collider program at Fermilab which ended in September 2011. The Recycler ring was equipped with four broad band barrier rf cavities capable of providing rf pulses of practically of any shape with a maximum amplitude of 2 kV [19] and a very versatile LLRF control to carry out varieties of rf manipulations [20]. The available bucket area for the beam stacking is in access of 250 eVs. However, the Fermilab collider demanded the beam to be cooled to less than about 70 eVs for its optimal operation. Normally, in access of 400×10^{10} antiprotons were stacked in the Recycler for collider use.

Testing of LPAC scheme in the Recycler was carried out in two steps. First, computer simulations using a multi-particle beam dynamics code, ESME [21], have been carried out to establish the rf manipulation steps. Then, experiments were done with proton beam in the Recycler to demonstrate the technique. Finally, the scheme is implemented operationally in the Recycler to check its compatibility with the rest of the collider program.

III.1 ***Simulations***

Figure 2 shows simulated beam particle distribution in ($\Delta E, \tau$)-phase space along with the barrier rf pulses for the LPAC scheme. The initial beam particle distribution was confined in a barrier bucket with pulse width and height of about 0.91 μsec and 1.93 kV, respectively, and the gap between the two rf pulses was about 5.89 μsec as shown in Fig. 2(a). In this case, we chose total phase space area of the initial beam stack to be about 108 eVs for illustration. The synchrotron period of the outer most particles in this distribution was about 1.6 sec. Before populating the new beam the initial beam is further confined in a mini-barrier bucket of total area equals 108 eVs inside the initial barrier bucket by opening it iso-adiabatically in about 12 sec, as shown in Fig. 2(b). The pulse height, gap and width of the mini-bucket were about 1.93 kV, 0.25 μsec and 5.4μsec, respectively. There is infinite number of combinations for the mini-bucket rf parameter, e.g., a combination of pulse height of 1.35 kV, pulse width of 0.36 μsec and pulse gap of 5.17 μsec also gives total phase space area of 108 eVs and can capture all beam in the initial stack. After the new beam arrives (see Fig. 2(c)) the barrier pulses separating the initial distribution and the newly arrived beam distribution are removed applying morphing technique; the width of the two rf pulses is continuously reduced keeping the length of the unstable region constant. We find that this sort of morph merging gives minimal emittance growth to the new beam. The longitudinal emittance of the new beam was taken to be about 7 eVs. By bringing the left most barrier pulse adjacent to the left rf pulse of the mini-barrier bucket completes the coating as shown in Fig. 2(d). The steps in Figs. 2(c) and 2(d) can be repeated as many times as needed. In this case the final emittance of the beam was found to be about 113 eVs; thus, the simulations showed negligible emittance growth. The simulations presented here have been carried out taking in to account of space charge force between beam particles and beam interaction with the beam pipe impedance and rf impedance of nearly 200Ω in the model.

The simulation clearly shows that the robustness of the scheme depends on the type of the initial particle distribution. For example if the initial distribution of particles in the tail regions, both in ΔE and in τ coordinates resemble parabolic or elliptic, then the coating can be performed with minimum or no emittance growth. However, if these distributions resemble Gaussian shapes then about 5% of the particles lie outside three-standard deviation.

Consequently considerable emittance growth is seen even if we carry out the rf gymnastics much more adiabatically as compared with the one illustrated in Fig. 2. The beam in the Recycler exhibits closer to logarithmic in ΔE and parabolic in τ coordinates due to combination of stochastic cooling [23] as well as electron cooling [24].

III.2 ***Experimental Demonstration***

The beam test was carried out in the Fermilab Recycler. The experiments were carried out using proton [14, 22] as well as antiproton beams. Here I illustrate the case with the antiproton beam. The measured wall current monitor data and the corresponding rf wave form at various stages of the beam manipulations are shown in Fig. 3.

Initial beam of about 2.56×10^{12} antiprotons were stored in a rectangular barrier bucket of T_2 =5.89 μsec, pulse width~ 0.91 μs each and pulse amplitude ~1.92 kV. The beam is cooled using stochastic cooling as well as electron cooling to a longitudinal emittance ~ 70±7 eV s (95%) . (Measured line-charge distribution and the Schottky data (energy distribution) for the initial beam are shown in Fig. 4(a) and 4(b), respectively (red traces)). Then, a mini-bucket of area ~66 eV s, (V_0 ~0.72 kV, pulse width~0.25 μsec and pulse gap ~5.4 μsec) was opened to capture about 95% of the initial beam. Corresponding measured line charge distribution and the rf wave form are shown in Fig. 3(a). Prior to new beam transfer to the Recycler, four 2.5 MHz rf buckets of total area of about 14 eV s are opened and about 14×10^{10} antiprotons of about 7±1 eVs are extracted from the antiproton source and have been injected into the already opened matched buckets of the Recycler as shown in Fig. 3(b). Finally, the newly arrived antiprotons are coated on previously captured antiprotons in the mini-barrier bucket without disturbing it. Figure 3(c) shows the wall current monitor data corresponding to the initial stages of beam coating soon after the 2.5 MHz rf waveform and the rectangular barrier pulses separating mini-bucket and newly arrived beam are removed. Completion of coating of the beam is shown in Fig. 3(d).

The measured wall current monitor and the Schottky data (red traces) for the beam after two more successive beam coating are shown in Figs. 5(a) and 5(b). These coating have been carried out by repeating the steps depicted in Figs. 3(b)-3(d) each time. The beam longitudinal emittances and beam intensities for these two transfers were 8±1 and 7±1 eV s 9×10^{10} and

5×10^{10} antiprotons each, respectively. The data shown in Fig. 5 corresponds to a total beam of 2.84×10^{12} antiprotons.

The barrier pulses seen by the beam in this experiment were not exactly rectangular in shape; the rise time and fall time for a rectangular barrier pulse was about 10 nsec. Also, there was a polar asymmetry for the barrier pulses; the negative pulses were a few percent smaller than the positive barrier pulses. The origin of this asymmetry for barrier rf pulses was identified to be non-symmetric saturation curves of the power amplifiers used in the Recycler rf system. Consequently, the longitudinal emittance could not be obtained using standard analytical formula given earlier, but, we had to use a beam Monte Carlo (MC) method [25]. We use the ESME code to construct the beam particle distribution in $(\Delta E, \tau)$ –space by matching simulated time and energy projections to the measured wall current monitor and Schottky data, respectively, as shown in Figs. 4 and 5. The longitudinal emittances for beam after three coats found to 100±10 eV s. These emittances represent phase space area occupied by 95% of the beam particles as indicated by blue curves in Figs. 4(c) and 5(c). Now if we add the emittances of the initial beam and that of the coated beam we find emittance dilution is less than 10%. By adding the errors in quadrature the observed emittance dilution is within measuremental errors of about 10% of the experiment.

Figure 6 shows the data from LPSC stacking scheme in the Recycler for regular operation. The dashed line separates a transition from "normal stacking" which involved only the morphing merging of the injected beam (potentially had high risk of longitudinal emittance growth for the dense region of the beam particle distribution because of complete removal of the rf pulse at the boundary of the initial beam) and the LPSC scheme. During this study LPSC scheme was used to stack beam from about 270×10^{10} antiproton to about 400×10^{10} antiproton in the Recycler. The shown measurement data are measured average transverse emittance $<\varepsilon_{\perp}>$, average beam brightness $< d >= N(\times10^{10})/[\varepsilon_{\perp}(\mu\text{m})\varepsilon(\text{eVs})]$ and antiproton beam intensity. Each step in intensity curve indicates a new set of beam transfer from the Fermilab antiproton source. Between two successive set of beam transfers the time gap was about forty five minutes and the beam was cooled mainly using stochastic cooling with about a few minutes of electron cooling. The inset in Fig. 6 is Schottky data measured soon after final beam coating but with mini-buckets removed. At the end of the beam stacking the antiprotons have been used for one of the collider

operation. We also had similar beam stacking, having LPSC scheme at the early part of the beam stacking till the beam intensity reached about 270×10^{10} followed by normal stacking to reach total intensity of about 400×10^{10}. In both cases the LPSC scheme was transparent to the rest of the collider operation. A comparison of the final distributions between normal stacking and that obtained from the LPSC showed similar behaviour within the measuremental errors. The central dense region of the beam distribution was disturbed very little even in case of normal stacking because the synchrotron oscillation period of the beam particles close to synchronous energy were in the range of several seconds. As a result of this, operationally we found little difference between these two techniques in the Recycler.

IV. Measurement of Incoherent Spectrum using LPSC

Mapping of the synchrotron frequency spectrum of particles in a standard sinusoidal rf bucket had been done before [26]. The LPSC method of beam stacking provides an elegant method to measure and map the synchrotron tune of beam particles in barrier buckets. The incoherent synchrotron frequency f_s of beam particles on the outermost separatrix of mini-rectangular barrier bucket is $f_s^{-1} = 2T_2\beta^2 E_0 / |\eta \Delta E_m| + 4T_0 |\Delta E_m| / eV_m$. Here a rectangular barrier bucket of pulse height V_0 =1.84 kV, pulse width $\hat{T}$ =0.9 μs and pulse gap T_2 =5.9 μsec. is chosen as the bucket of interest to map the synchrotron frequency spectrum. Then a mini-bucket is grown inside the main bucket utilizing the entire pulse gap T_2. During this rf manipulation the rf bucket of interest was kept empty. Using the proton beam the empty mini-bucket was coated following the same steps as shown in Fig. 1. This created a long bunch with an ideal hole in the center. The separatrix of the mini-bucket acts as the boundary between the empty region and the coating. The wall current monitor signal is fed to Agilent 89441A 2.65GHz VSA (with a frequency span of 0-4Hz, centered at the RR revolution frequency) to measure synchrotron frequency of the particles sitting on the separatrix. By changing the mini-bucket parameters of the mini-bucket the entire synchrotron spectrum is scanned. The ΔE_m in each case is measured using Schottky measurement. The measured synchrotron frequency as a function of ΔE_m is shown in Fig. 7 along with analytical predictions assuming ractangular barrier pulses. The level of descripancy between measurements and the predictions of synchrotron frequency spectrum

can be understood as due to the shapes of rf pulses used in the experiment versus that used in calculations.

During each of the measurements mentioned above a hollow bunch is created. However, the hole in the longitudinal phase space is maintained by means of mini-bucket. We found that even in the absense of mini-barrier bucket a clean hollow beam can be maintained as shwn in Fig. 8. We certainly observe some leakage of beam particles into the hollow region manily because of non-adiabaticity of the rf manipulation while removing the mini-bucket. No degradation in hollow beam is seen even after a long time (of the order of hours). Figures 8 (a) and (b) show measured and ESME predicted line-charge distributions for the hollow beam. The corresponding beam particle distribution in the longitudinal phase-space is shown in Fig. 8(c). We see quite good agreement in the predictions and the measurement data.

At this time, hollow beams are of purely of academic interest. The hollow beam of the type explained here may be of very high interest from the point of view of studying varieties of distribution functions and studying beam physics.

V. Summary

We have proposed and validated a novel beam stacking method, longitudinal phase space coating, for a storage ring using rf barrier buckets. The scheme has been studied using multi-particle beam dynamics simulations and the technique has been demonstrated with beam experiments in the Recycler. This method has been successfully implemented and is used operationally for antiproton beam stacking. We have demonstrated the ability of this technique to antiproton stacking with less than 10% emittance dilution. The method works in such a way that the majority of the central region of the phase space is undisturbed throughout the stacking.

The rf gymnastic features to the longitudinal phase space coating is quite useful in measuring the incoherent synchrotron spectrum of the beam distribution in a barrier bucket. We illustrated such measurement on one typical barrier bucket used at the Recycler. The measurement data is reproduced quite well by an analytical calculation. This technique is used to create an ideal hollow beam in longitudinal phase space.

As a final note, we expect that the applications of the technique described here for phase space coating isolating dense region of a phase space not be unique to high-energy storage rings for protons and antiprotons. The technique developed here that use barrier rf will be very useful

in heavy ion storage rings and it should have broad application in other low energy circular storage rings.

Acknowledgements

The author would like to thank D. Neuffer and D. Wildman for many useful discussions. Special thanks are due to the Fermilab Accelerator Division MCR crew. This work is supported by Fermi Research Alliance, LLC under Contract No. DE-AC02-07CH11359 with the U.S. Department of Energy.

References

[1] 'Injection',G. H. Rees, CAS, CERNREP / 94-01_v2, p 731.

[2] Design Report "National Accelerator Laboratory", 2nd printing, 1968; J. P. Blewett, BNL Accelerator Dept. Report AADD-169 (CRISP 71-6), 1971; E, D. Courant, CRISP 71-5, 1971.

[3] A. G. Ruggiero, Fermilab-TM-498, (1974); C. Ankenbrandt, Fermilab-FN-352-0400.00, (1981), S. Shukla, *et. al*, PAC1997, (1997) p 144; K. Seiya, *et. al*, PAC07 (2007), p 742.

[4] K. R. Symon and A. M. Sessler, in: Proc. of the CERN Symposium on High Energy Accelerators (CERN, Geneva, 1956), p. 44-58; S. Van der Meer, IEEE Trans. on Nucl. Sci., Vol 28, No. 3 June 1981, p. 1994.

[5] M. Benedikt and S. Hancock, Nucl. Inst. Methods A 550 (2005) 1-5.

[6] D. W. Hudgings and A. J. Jason, Proc. 11th Int. Conf. on High Energy Accel., Geneva (1980) pp. 277-282; Y. Kamiya,, PAC89 (1989), page 2843 ; Y. Y. Lee, M. Blaskiewicz, A. Fedotov, D. Raparia, J. Beebe-Wang, W. T. Weng and J. Wei, Proc. of LINAC2002(2002) p 67 ; L. Liu, J. Qiu, J. Tang, T. Wei, PAC09 (2009) p1403.

[7] G. Jackson, Fermilab-TM-1991, November, 1996.

[8] J.E. Griffin et al., IEEE, Trans. Nucl., Sci., NS-30, 3502 (1983);

[9] S. Y. Lee, Accelerator Physics, **1**st edition (World Scientific, Singapore, 1999), Chap. V, p.305; S.Y. Lee and K. Y. Ng, Phys. Rev. E, Vol. 55, 5992 (1997); K. Y. Ng, Phys. Rev. ST Accel. Beams 9, (2006) 064001; J. Griffin, "Momentum Stacking in the Main Injector

using Longitudinal Barriers," (unpublished) 1996; K. Y. Ng, Phys. Rev. ST Accel. Beams 5, (2002) 061002;

[10] M. Fujieda, et. al., Phys. Rev. ST Accel. Beams 2, (1999) 122001; K. Takayama et. al., Phy. Rev. Lett. 8 (2002) 144801-1; K. Takayama et. al., RPIA2006, KEK Proceedings 2006-12, January 2007, p 1; K. Takayama et. al., Phys. Rev. Lett. 98, 054801 (2007); Y. Shimosaki, et. al.,Phys. Rev. ST Accel. Beams 7, (2004) 014201.

[11] O.Boine-Frankenheim and I. Holfmann, Phys. Rev. ST Accel. Beams 6, (2003) 034207; O.Boine-Frankenheim, Phys. Rev. ST Accel. Beams 13, (2010) 034202.

[12] M. Blaskiewicz et., al., Proc. of PAC99, New York, page 2280; M. Blaskiewicz, BNL AGS/AD/Tech. Note No. 409 (January 13, 1995); M. Blaskiewicz, AIP Conf. Proc. 377 (1996) p 283; T. Bohl, T. Linnecar, E. Shaposhnikova EPAC2000 (2000) p1200.

[13] C. M. Bhat, Phys. Lett. A 330 (2004), p 481.

[14] C. M. Bhat, RPIA2006, KEK Proceedings 2006-12, January 2007, p 51 (and FERMILAB-CONF-06-102-AD and references therein); C.M. Bhat, FERMILAB-FN-0916-AD (2011) and references therein.

[15] C. M. Bhat, B. E. Chase, C. Gattuso, P. W. Joireman, Proc. of PAC07 (2007) 1941; P. W. Joireman and B. E. Chase (private communications 2006).

[16] L. R. Prost, A. Burov, A. Shemyakin, C. M. Bhat, J. Crisp, N. Eddy, FERMILAB-TM-2498-AD; C.M. Bhat and K.Y. Ng, FERMILAB-CONF-03-395-t-(2003); T. Sen, C.M. Bhat, and J.-F. Ostiguy, FERMILAB-TM-2431-AD (2009); A. Smirnov, A. Sidorin, D. Krestnikov, C. Bhat, L. Prost, COOL09 (2009) p 142; A. Shemyakin, C. Bhat, D. Broemmelsiek, A. Burov, M. Hu, COOL07 (2007) p 171.

[17] C. Dimopoulou, K. Beckert, P. Beller,* A. Dolinskii, U. Laier, F. Nolden, G. Schreiber, M. Steck, and J. Yang, Phys. Rev. ST Accel. Beams 10, (2007) 020101.

[18] C.M. Bhat, Beams-Doc-2057-V1, December 2005; C. M. Bhat, EPAC2008 (2008), p 307; C. M. Bhat, IPAC2011 (2011), p 2763.

[19] J. E. Dey and D. W. Wildman, PAC1999, p 869; (also private commutations with Dave Wildman and Joe Dey).

[20] "Current DSP Applications in Accelerator Instrumentation and RF", B. Chase, A. Mason, and K. Meisner, ICALEPS'97 (1997) (unpublished) http://www.aps.anl.gov/News/Conferences/1997/icalepcs/paper97/p230.pdf;

P. Joireman, B. Chase and K. Meisner, since 2004 a significant improvement is made in RRLLRF (private communications).

[21] J. A. MacLachlan, HEACC'98, Int. Conf. on High Energy Accelerators, Dubna, Sept. 1998; J. A. MacLachlan, Fermilab Report No FN-529, (1989) (Unpublished); http://www-ap.fnal.gov/ESME/.

[22] C.M. Bhat, Beams-Doc-2057-V1, December 2005; C. M. Bhat, KEK Proceedings 2006-12, January 2007, p 51.

[23] D. Broemmelsiek, M. Hu and S. Nagaitsev, EPAC2004 (2004), p 794.

[24] Sergei Nagaitsev, Daniel Broemmelsiek, Alexey Burov, Kermit Carlson, Consolato Gattuso, Martin Hu, Thomas Kroc, Lionel Prost, Stanley Pruss, Mary Sutherland, Charles W. Schmidt, Alexander Shemyakin, Vitali Tupikov, Arden Warner, Grigory Kazakevich, and Sergey Seletskiy, Phys. Rev. Lett. 96, (2006) 044801.

[25] C. M. Bhat and J. Marriner, PAC2003 (2003),p 514.

[26] H. Huang et. al., Phys.Rev.E48-4678(1993).

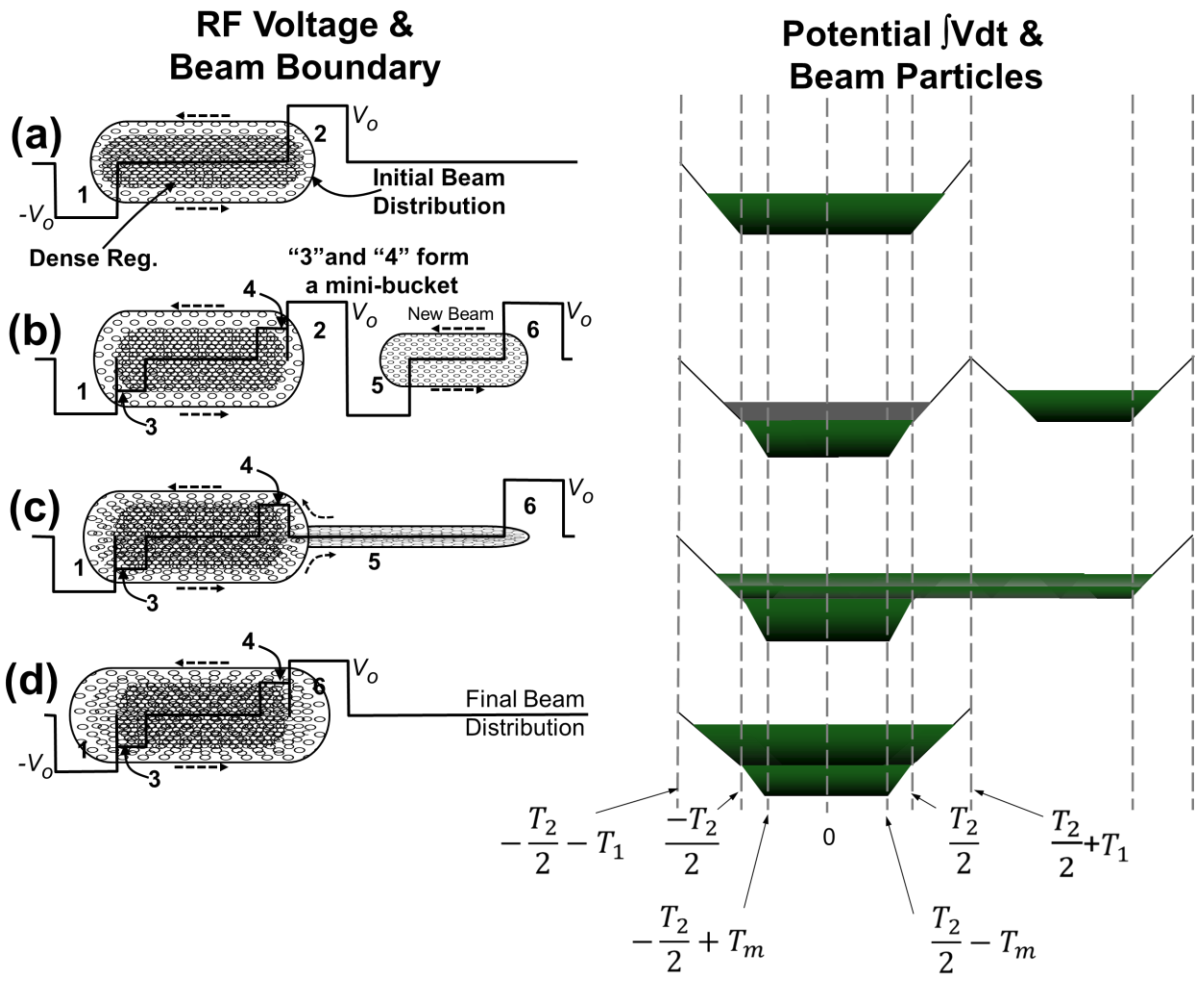

Figure 1: Schematic view of beam stacking by LPSC. The phase space (left) and potential diagrams (right) are shown for every stage of stacking: (a) original beam, (b) after capturing the dense region of the original beam in a mini-barrier bucket and injection of a new beam, (c) first stage of coating of the new beam on top of the original beam and (d) after coating. The voltage wave forms (solid lines) and direction of the synchrotron motion of the beam particles in (ΔE, Δt) phase-space are also shown in each case. The horizontal line indicates time axis.

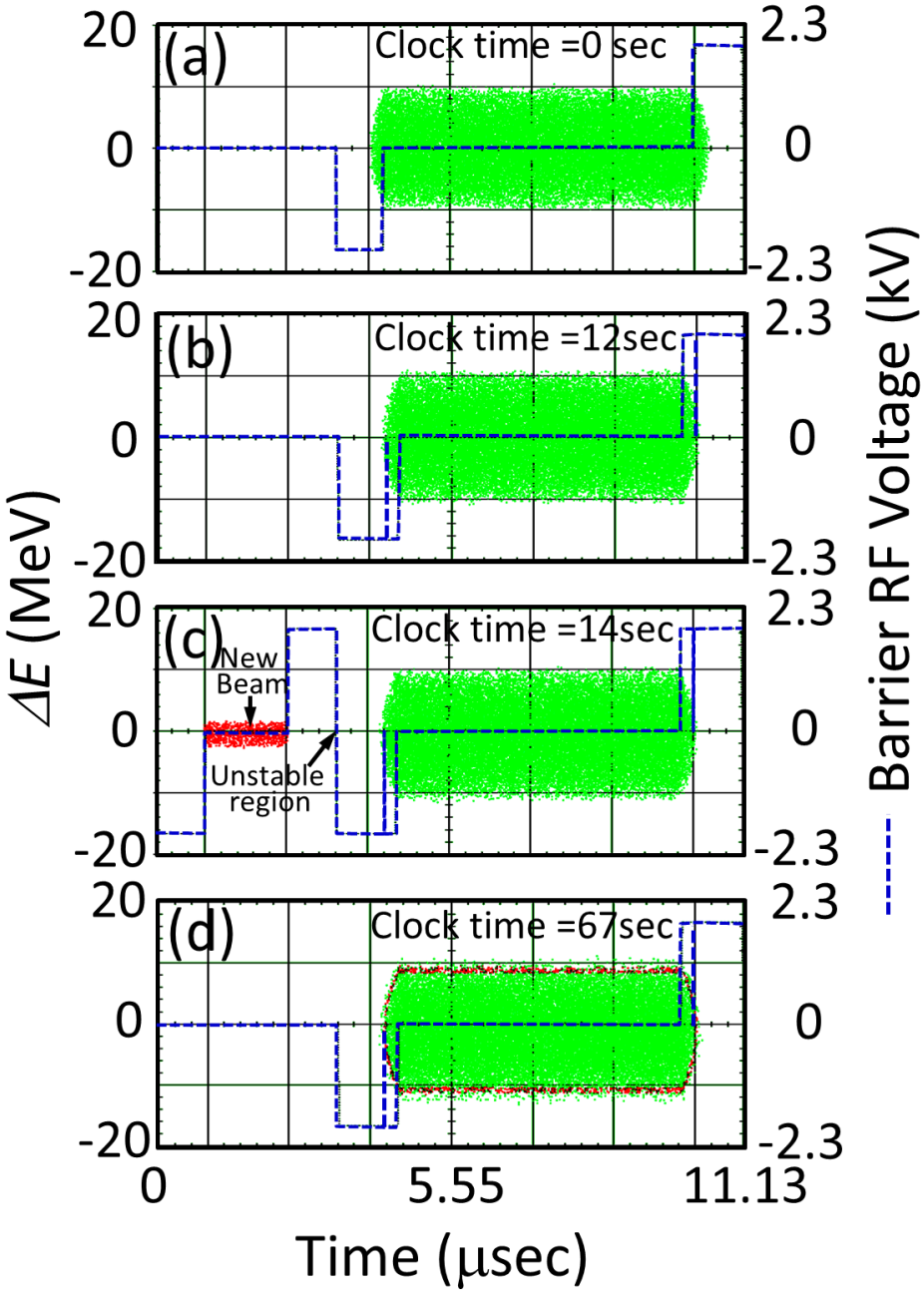

Figure 2: Simulated barrier rf wave form (blue dashed curve) and the ($\Delta E, \Delta t$) phase-space distributions of protons in the Recycler for (a) initial distribution, (b) after opening a mini-barrier bucket with pulse length of 0.25 μsec, which can capture all beam particles, c) injection of new beam with longitudinal emittance of about 7 eVs and d) after coating the new beam on the initial beam. Total clock time used to perform the rf manipulations are also shown.

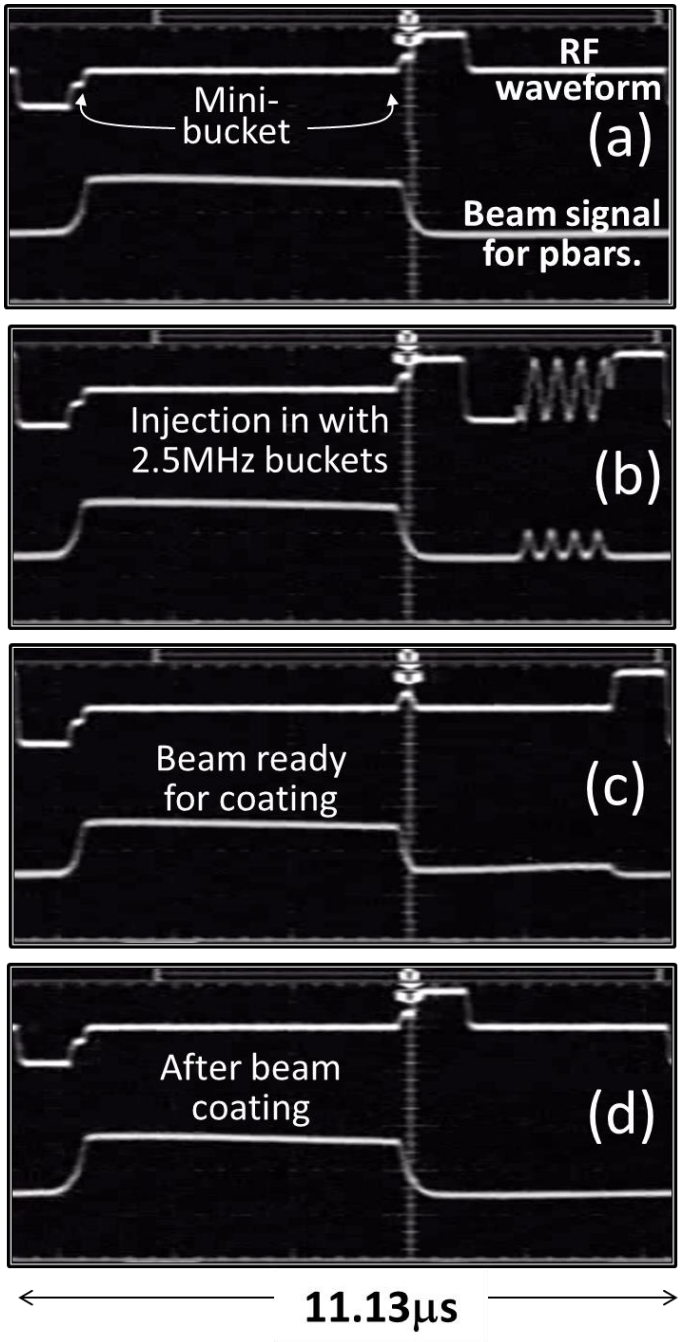

Figure 3: The scope pictures for the longitudinal phase space coating in the Recycler. The two traces in each of the figures represent rf wave form (top trace) and beam signal from wall current monitor (bottom trace). The stages of the coating are shown.

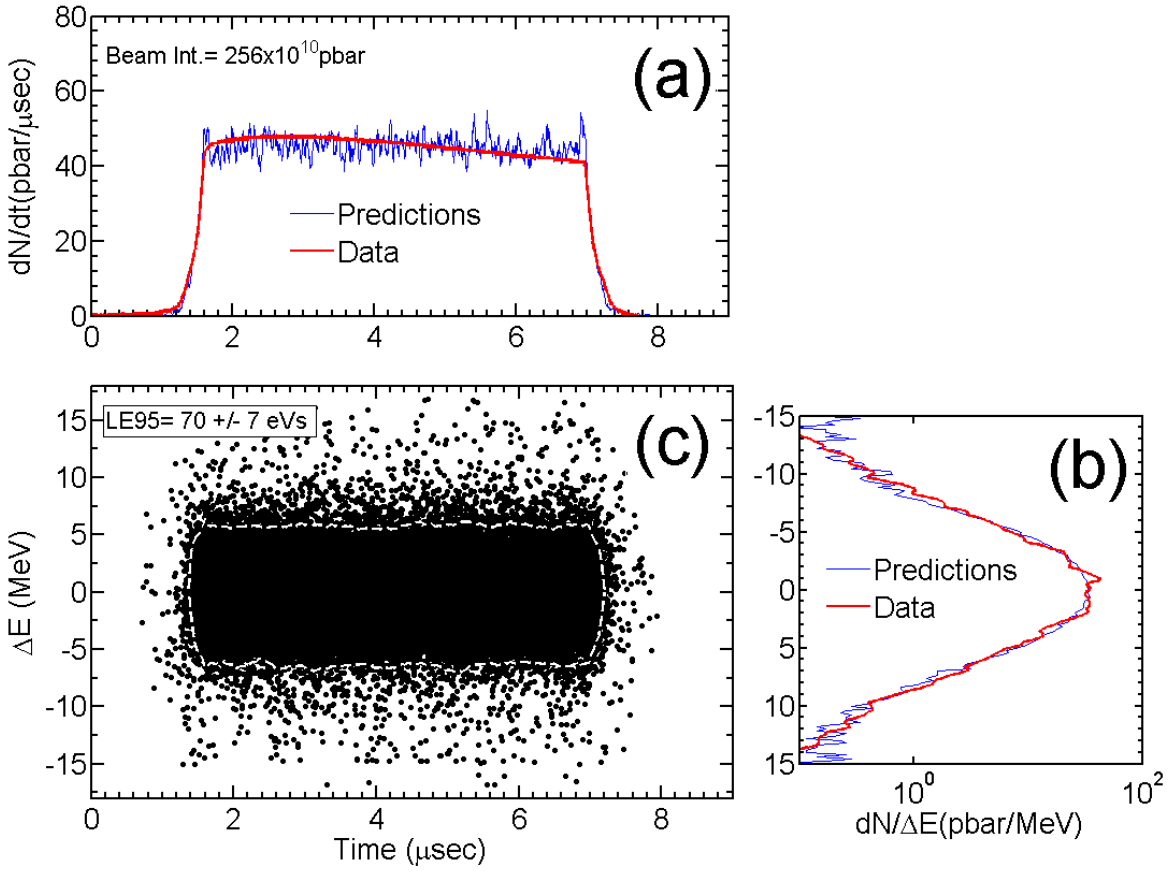

Figure 4: Comparison between ESME simulations with the measurement data for the initial beam. LE95(initial beam)≈70±7 eVs. The denser region of the initial beam occupying about 66 eV-s of the longitudinal phase space is captured using a mini-barrier bucket. The rest are retained in the outer barrier bucket. (a) Wall current monitor and (b) Schottky detector data. The blue and red traces are, respectively, experimental data and simulations. (c) The simulated longitudinal phase-space distribution of the beam with 95% contour.

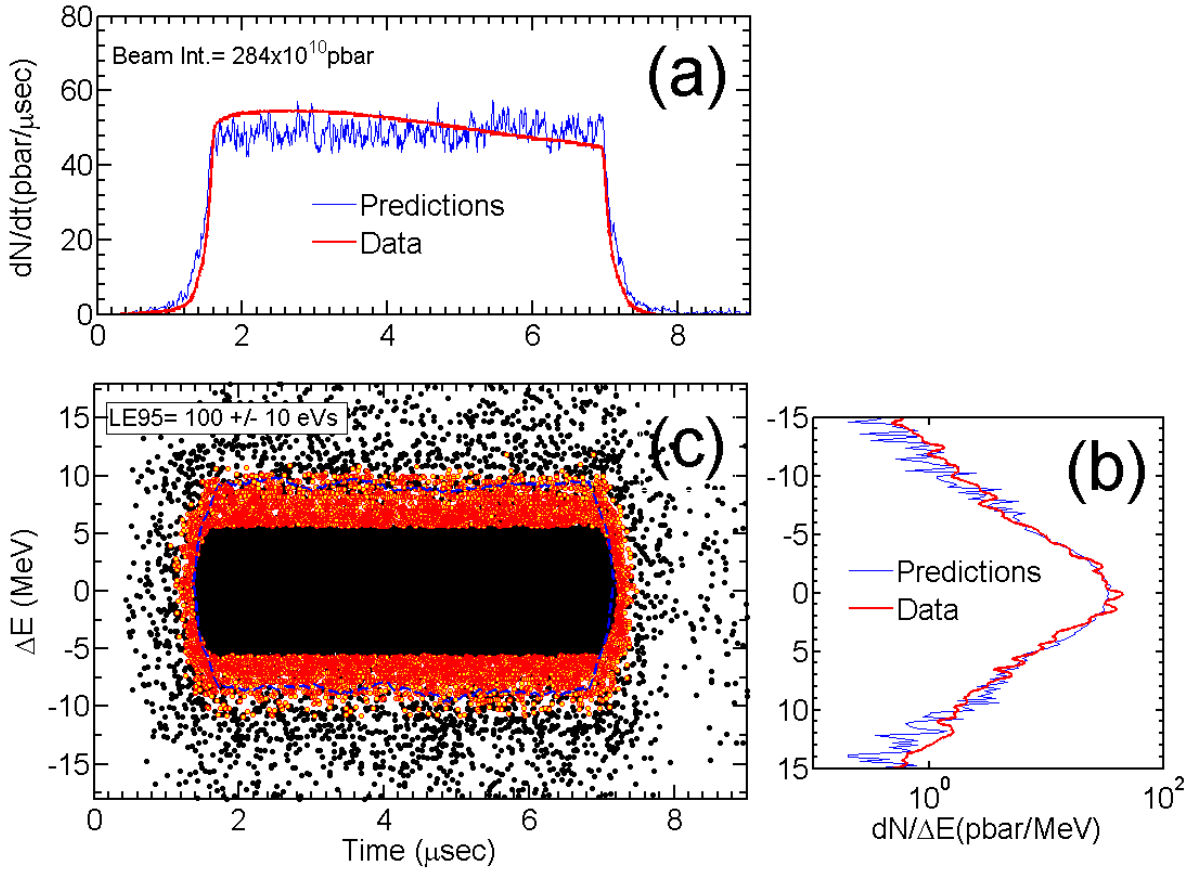

Figure 5: Comparison between ESME simulations and the measurement data for the pbar beam after three coats. The descriptions for three plots and the traces are the similar to that in Figure 2. The beam captured using the mini-barrier bucket can be seen clearly in the middle.

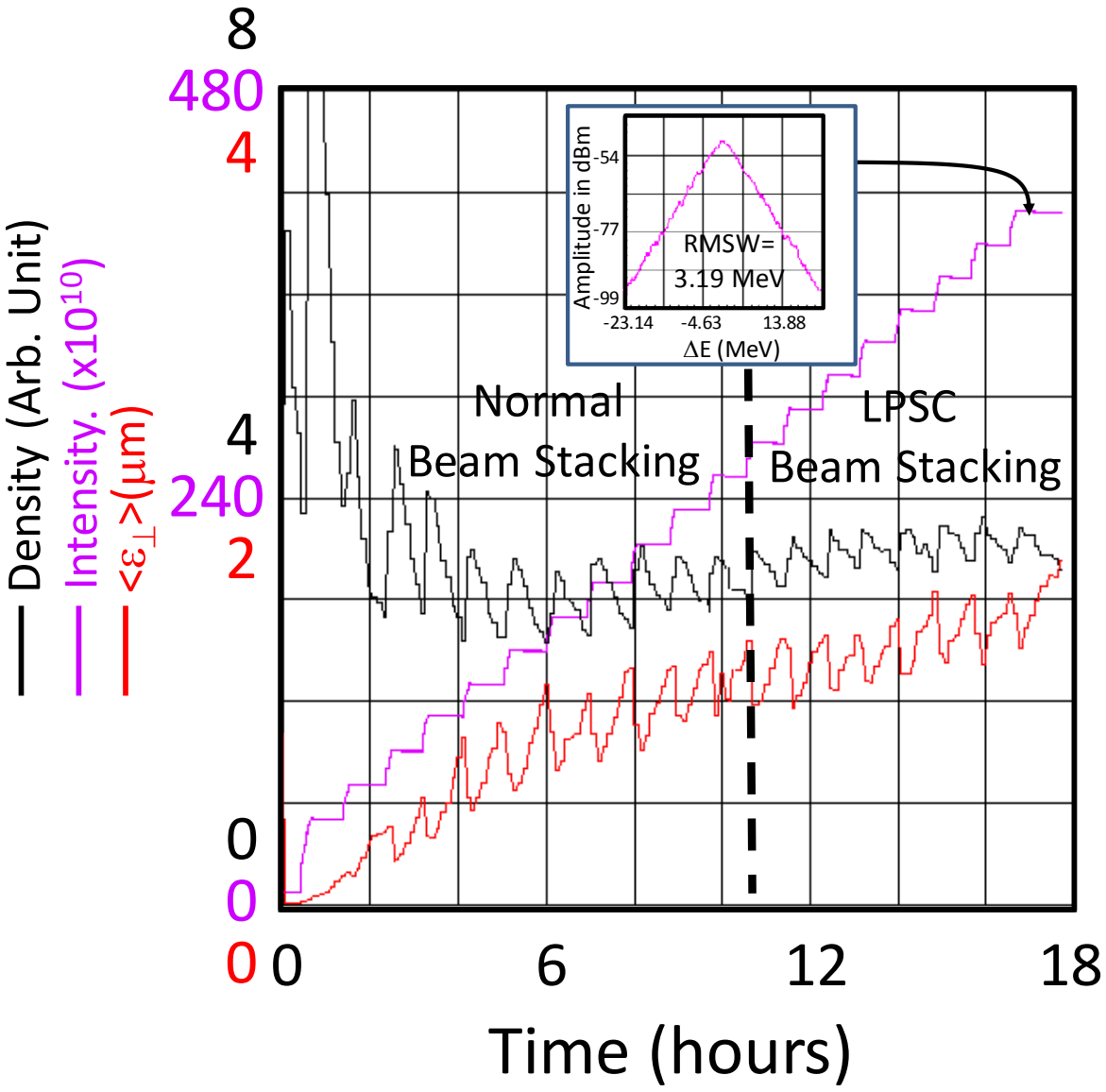

Figure 6: Antiproton stacking before and after implementation of LPSC scheme in the Recycler. Black curve is a measure of brightness of the beam in units of ($\times 10^{10}$pbars/μm/eVs). Magenta curve is beam intensity and red curve is the measured transverse emittance. The dashed line represents transition from standard beam stacking and the longitudinal phase space coating.

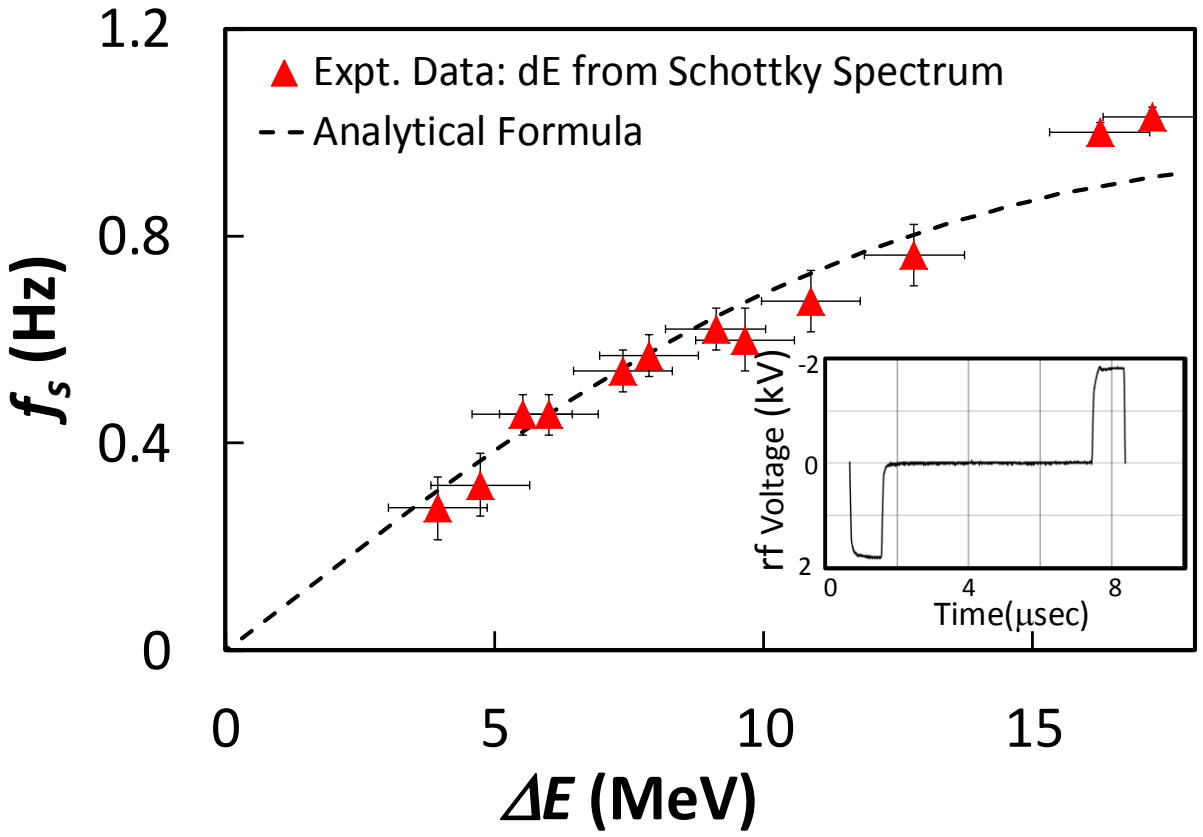

Figure 7: Measured and calculated synchrotron frequency as a function of $\hat{\Delta E}$ of beam particles in a RR barrier bucket with V_0=1.83 kV, $\hat{T}$=0.9 μs and T_2=5.9 μs. The dashed line is obtained with analytical formula assuming ractangular barrier waveform. The inset shows exact rf waveform used in the measurement.

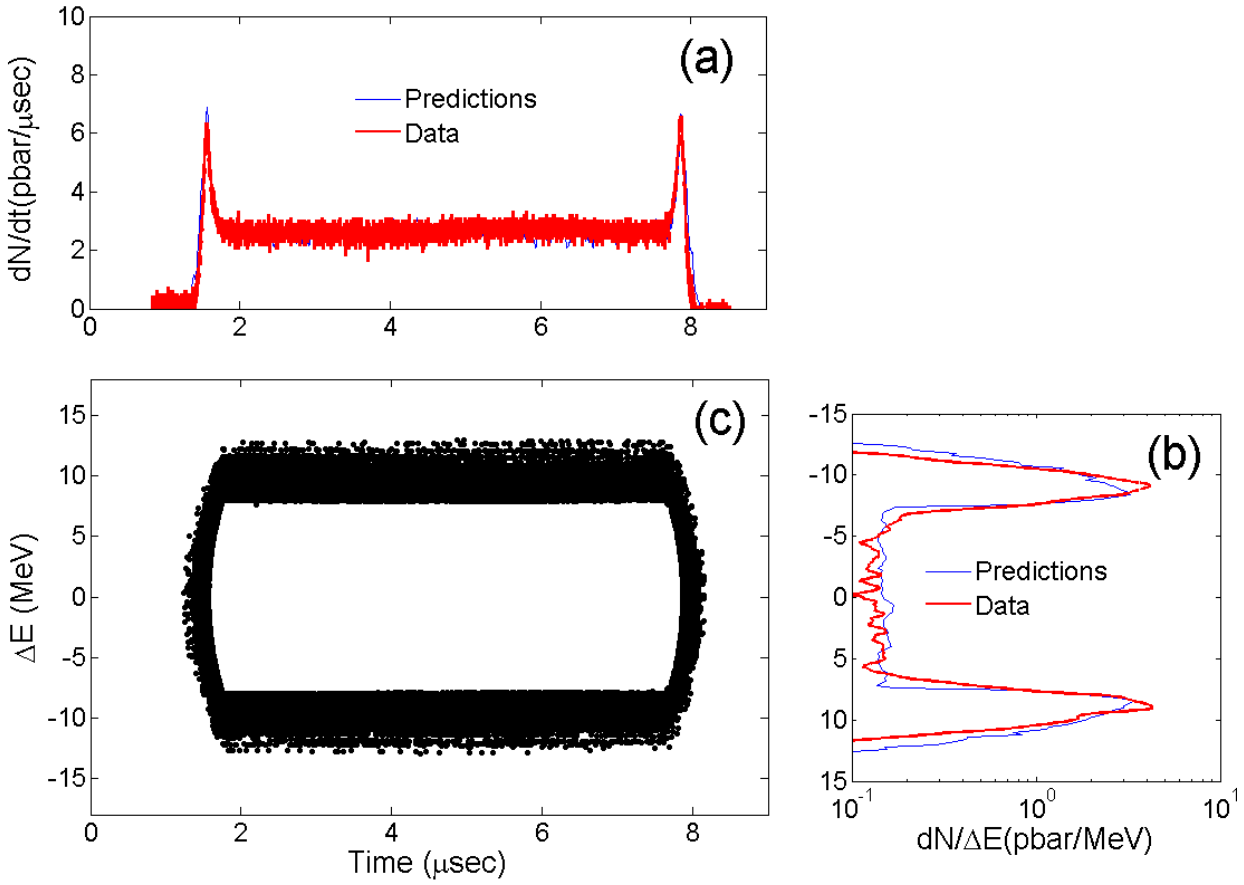

Figure 8: (a) Measured (red curve) and ESME predicted (blue curve) line-charge distribution, (b) Measured Schottky (red curve) and ESME predicted energy projection (blue curve) and (c) predicted longitudinal phase-space distribution for a typical hollow beam with about 18×10^{10}p in the Recycler.